Journal of the European Ceramic Society 41 (2021) 1332–1341

Contents lists available at ScienceDirect

Journal of the European Ceramic Society

journal homepage: www.elsevier.com/locate/jeurceramsoc

Original Article

Influence of the experimental set-up and voltage ramp on the dielectric breakdown strength and breakdown site in borosilicate glass

Pia-Kristina Fischer, Gerold A. Schneider *

Institute of Advanced Ceramics, Hamburg University of Technology, Denickestraße 15, 21073 Hamburg, Germany

ARTICLE INFO

Keywords:
Voltage ramp dependence
Dielectric breakdown strength
Initialization site
Breakdown location
Electrode configuration

ABSTRACT

The dielectric breakdown strength of borosilicate glass and alumina was measured as a function of the voltage ramp rate on different material thicknesses and with different electrode configurations. While this is not a completely new approach, with our work we want to highlight the importance of appropriate measurement set-up and contribute to a better understanding and analysis of dielectric breakdown. The measurement of breakdown tests is generally anything but trivial and the comparison of breakdown results for different set-ups is difficult, especially because not all scientific articles go into detail on the measurement method and all the important parameters, which can influence the breakdown event. For the results shown in this work we mainly used glass as a suitable model material and two different electrode setups at eleven different voltage ramps in the range of 5 V/s to 10,000 V/s. We found that there is a clear dependence of the dielectric breakdown strength on the voltage ramp and the electrode configuration as well as it should be distinguished between breakdowns which initiated at electrode edge and those initiated within the electrode area. There is almost no scatter for breakdown strengths which were initiated inside a silver paste electrode in comparison to breakdown strength from the electrode edges.

1. Introduction

Dielectric breakdown (BD) is a critical and limiting event/factor which may lead to catastrophic damage in electrical and electronical devices. Defined as the maximum voltage divided by the material thickness an insulator can withstand, dielectric BD was investigated from the 1920s on by von Hippel who developed a first electron avalanche model [1–3]. Fröhlich extended the model of von Hippel by the so-called "low energy" criterion [4,5]. In parallel, continuum theoretical thermal BD models by Fock [6], Moon [7] and Wagner [8] were developed and the electromechanical breakdown model for thermoplastic polymers by Stark and Garton [9] later on modified by Fothergill [10] to a filamentary electromechanical breakdown model. These models have been taken up repeatedly over the years and adapted for specific applications (by e.g. Klein and Gafni [11] and enhanced by e.g. O'Dwyer [12,13] or Sparks [14], Budenstein [15] or McPherson [16]). Based on von Hippels avalanche model, by applying density function perturbation theory Sun et al. [17,18] succeeded convincingly to predict the intrinsic breakdown for covalently bonded and ionic materials. Until more recently, BD models were developed in analogy to fracture mechanics [19–28].

But still after decades of investigations dielectric breakdown mechanism is by far not fully understood and researchers and developers have to deal with a lack of comprehensive data. Consequently, breakdown strength of insulators is still empirically optimized due to a missing generally accepted macroscopic model, which is able to predict the dielectric breakdown correctly.

It is well known that, besides the microstructural defects [29–33], the experimental conditions of the electric breakdown test setup influence the measured breakdown strength of a material substantially [34–39], which was just recently confirmed by measurements of Mieller [40]. Although standards exist [41–44], these do not prescribe the exact measurement method and within their framework differences of up to 50 % were measured for the same material [40]. This makes it difficult to compare data from different sources, especially when not all the detailed test conditions and observations are documented and stated/reported in the scientific articles. Among them a key parameter, whether the breakdown initiates at electrode edges or within the electrode, is usually not reported.

Concerning the size dependence of dielectric breakdown there exists

* Corresponding author.
E-mail address: g.schneider@tuhh.de (G.A. Schneider).

https://doi.org/10.1016/j.jeurceramsoc.2020.09.060
Received 21 July 2020; Received in revised form 21 September 2020; Accepted 25 September 2020
Available online 28 September 2020

a lack of data because most often breakdown experiments are performed on thin films below 1 μm thickness whereas on thick films and bulk materials much less data are available. For the dielectric breakdown in thin films there is a lot of literature where the physical phenomenon, structural damage, breakdown statistics, device reliability and technological implications are extensively discussed [45–47]. SiO_2 is studied intensively because of its great use in MOS and MIM devices [48] but as mentioned above it is almost all about thin films where intrinsic dielectric BD prevails. But it is clear that the breakdown mechanism changes from an intrinsic to an extrinsic one around 1 μm and 20 μm thickness [49]. However, in thin films it has been shown that intrinsic breakdown can be predicted by Von Hippels Avalanche Model [18] for different non-metals, semi-metals and metal halides. For the extrinsic breakdown mechanism in thick films and bulk materials there is no commonly accepted model [49].

The objective of this study is to contribute to the understanding of the dielectric breakdown mechanism by studying the influence of voltage ramp rates on the dielectric strength and to emphasize the importance of a comprehensive and detailed report of the test conditions.

We chose glass for our investigations, since it is assumed and partially shown, that microstructure influence the dielectric breakdown strength, because pores, grain boundaries, impurities, crystallographic defects and secondary phase could act as charge traps [29,30,32,33,50]. Glass as an amorphous material is homogeneous without grain boundaries or crystal orientations and therefore measured differences in the breakdown strength and breakdown morphology can be attributed to the electrodes and the voltage ramp. Furthermore, silica is of great use in micro-electric devices such as integrated circuits (ICs), wafers and MEMS [51,52] which makes it the perfect model material for this purpose.

2. Material & methods

2.1. Sample preparation

For the investigations in this work two different commercially available borosilicate glasses with relative permittivities of 4.4 ± 0.3 and 7.4 ± 0.3 were used, one of it in three different thicknesses. In the following they are named Glass A and B and details are given in Table 1.

Additionally, some experiments were also carried out on alumina samples custom made at our institute. The alumina powder (CT 3000 SG, Almatis) was pressed in the shape of discs by uniaxial and additional cold-isostatic pressing. Afterwards the green bodies were sintered at 1590 °C in air for one hour in a chamber furnace. The density of the sintered specimens was determined by Archimedes principle and resulted in 99 % relative density, ensuring a dense material. The sintered bodies were ground plan-parallel to the desired thickness by a flat-bed grinding machine (Table 1).

Table 1
Summary of the main characteristics of the different glass substrates and alumina. [53–55].

	Glass A	Glass B	Al_2O_3
Material	Borosilicate glass 3.3, Th. Geyer	Borosilicate glass D263 M, Thermo Scientific	CT 3000 SG, Almatis, powder
Composition	80.6 % SiO_2, 13.0% B_2O_3, 4.0% Na_2O & K_2O, 2.4% Al_2O_3	64.1% SiO_2, 8.4% B_2O_3, 6.4% Na_2O, 6.9% K_2O, 5.9% ZnO, 4.2% Al_2O_3, 4.0% TiO_2, 0.1% Sb_2O_3	99.8% pure Al_2O_3
Nominal thickness	152 ± 8 μm *	72 ± 1 μm, 152 ± 3 μm, 214 ± 5 μm *	503 ± 15 μm*
Dimension	24×32 mm^2	24×24 mm^2	Ø 28 mm
Density	2.23 g/cm^3	2.51 g/cm^3	3.95 g/cm^3 *
Relative Permittivity	4.4 ± 0.3 *	7.4 ± 0.3 *	9.8 ± 0.6*
Loss factor tan δ	0.016 *	0.025 *	0.005 *

*own measurements.

The thickness d of all samples was chosen to be in the sample thickness dependent extrinsic BD regime $d > 30\mu m$ according to [49] where the dielectric BD strength E_{bd} is proportional to $1/\sqrt{d}$.

All substrates were cleaned with ethanol, dried at 60 °C and every sample thickness was measured. According to DIN 53 483 the relative permittivity of the three materials was determined.

Since tests with different electrode configurations were conducted on some samples conductive silver paint electrodes were added which is described in detail in the following chapter.

2.2. Breakdown measurements

For all breakdown tests the same voltage source and measuring cage/chamber was used, only the electrodes directly connected to the samples were changed. The used voltage source is a ER75P4, Glassman high voltage Inc., UK, which can apply up to 75 kV. The samples were placed between two (rod-) electrodes and clamped by a spring force in a silicone oil bath in a custom-made test setup. For piloting and recording of the signals (storing voltage, time and current in one file) a LabVIEW-program was used. The DC voltage was increased linearly with different ramps between 5 and 10,000 V/s from 0 V until dielectric breakdown indicated through a collapse of the voltage signal and a sudden current flow. However, the current is limited to 2 μA to protect the whole measurement assembly. As the voltage is detected every 250 ms the accuracy of the breakdown voltage U_{bd} is between 0.004 % (for the 5 V/s-ramp, $U_{bd} \approx 30$ kV) and 5.00 % (for the 10,000 V/s-ramp, $U_{bd} \approx 50$ kV) and varies in absolute values between 1.25 V and 2500 V corresponding to the set voltage ramp. Additionally, the breakdown event was always accompanied by a low but hearable noise and a dark spot on the surface – the breakdown channel. The highest voltage reached before the collapse is defined as the breakdown voltage U_{bd}, which gives divided by the sample thickness the dielectric breakdown strength E_{bd}.

The breakdown tests were conducted with voltage ramps of 5, 10, 20, 50, 100, 200, 500, 1000, 2000, 5000 and 10,000 V/s. The 5000 V/s meets the standards [41,42] the breakdown to happen within 10–20 seconds. 500 V/s is recommended by the ASTM [43,44]. The slower ramps are performed to study the ramps dependency of the dielectric breakdown.

Two different electrode setups were used for the investigation of the voltage ramp impact/influence. For the first setup a three-electrode-configuration is used, shown in Fig. 1 a) and in the following called test setup A, which is often used for conductivity measurements. The material of all components is stainless steel. The positive HV-source is connected to a rod electrode with a diameter of 6 mm. The counter electrode, which is the ground or cathode, had a diameter of 18 mm and the ring electrode had an inner diameter of 20 mm. This ring-electrode is surrounding the ground electrode to avoid surface currents. For the second setup conductive silver paste (CSP) was applied as circular electrodes on both sides of the specimens. These silver paint electrodes had different sizes of 10 mm and 18 mm diameter on the top and bottom side, respectively, to avoid overlapping electric field enhancement at the electrode edges and thus a preferred but undefined breakthrough spot/area. The sample with its CSP-electrodes was then clamped between a rod electrode with a rounded end and a flat Rogowski-like electrode, illustrated in Fig. 1 b) and in the following called test setup B. The smaller one functioned here as the ground electrode (at zero potential) and the bigger one was connected to the positive HV-source.

For each setting minimum of five measurements were made. If one or more samples gave a value which differed by more than 15 % from the mean, five additional measurements were made.

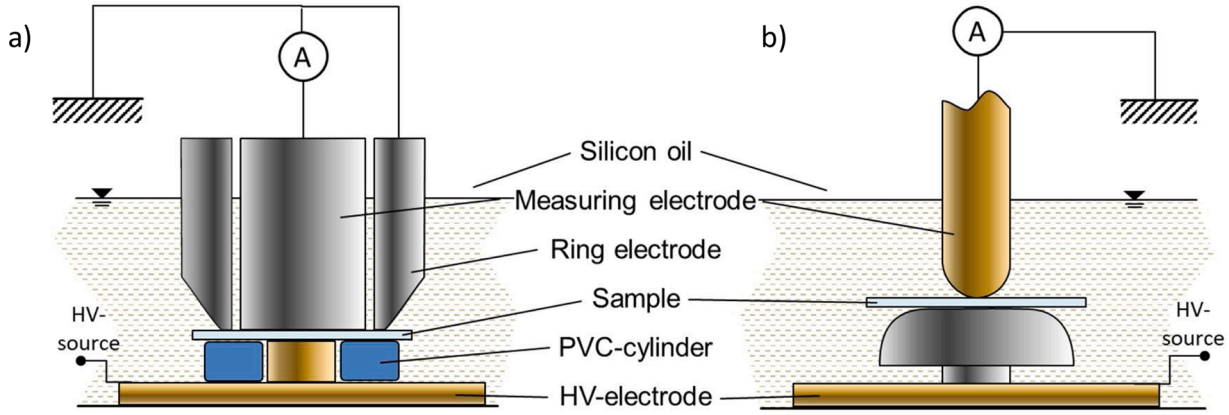

Fig. 1. Schematic illustration of the measuring setup until breakdown for the measurements a) with a three-electrode configuration (setup A) and b) the breakdown measurements with the sample clamped between a pin and a Rogowski-like electrode (setup B).

Additionally, breakdown measurements according to known standards were conducted to set the gained results in relation. For this purpose ten measurements were run with two opposing flat rod electrodes of 6 mm diameter at a voltage ramp of 500 V/s [43,44], called test setup C. Also ten samples were tested at 5000 V/s with a ball electrode and an opposing flat cylindrical electrode of 25 mm diameter [41,42], called test setup D. This setup was for comparison with the ASTM in addition tested at 500 V/s. In Table 2 an overview of the conducted measurements is listed.

After the breakdown tests some samples were cleaned with ethanol and sputtered with a 5 nm gold layer for SEM imaging with a Supra VP 55, Zeiss. Pictures of the breakdown channels were taken at an accelerated voltage of 2.0 kV and a working distance of 5.9 mm.

3. Results

After each measurement each individual specimen was checked for the expected breakdown channel. All tests showed breakdown channels accompanied by micro- and macrocracks and a black spot of decomposed material was visible. Additionally, the breakdown event is always accompanied by noise and light emission, which was clearly observable. Fig. 2 shows characteristic breakdown channels in Glass A. In 2a) a high magnification of the "black spot" depicts the entry hole of the breakdown. The burned, black material was cleaned away during sample preparation for this picture. The cross section in Fig. 2b) was obtained by simply breaking the sample. Unfortunately the glasses never broke through the middle of the channel. This is the reason why the channel seems to have a smaller diameter in cross-section.

Table 2
Overview of the conducted experiments under different test conditions and electrode configurations.

Test setup	Electrode configuration	Material	Thickness [µm]	Ramps [V/s]	No. of samples
A	Three-electrode-setup (Fig. 1 a), no CSP	Glass A	152 ± 8	all	5 or 10
		Glass B	72 ± 1	all	5 or 10
B	Pin-Rogowski electrodes (Fig. 1 b), with CSP-electrodes	Glass A	152 ± 8	all	10
			72 ± 1	all	5
		Glass B	152 ± 3	200	10
			214 ± 5	200, 2000, 5000	10
		Al_2O_3	503 ± 15	5, 200, 2000	10
C	Two rod electrodes (according to ASTM), no CSP	Glass A	152 ± 8	500	10
D	Ball on plate (according to DIN), no CSP	Glass A	152 ± 8	500 and 5000	10

Dielectric breakdown strength calculated from the breakdown tests at different voltage ramps is shown in Fig. 3. In Fig. 3a) the results for Glass A with the three-electrode setup A and the two-electrode setup with CSP-electrodes (setup B) are plotted. Different trends for the same material are observed. The three-electrode setup A gives significantly lower values than CSP-electrode setup B. Furthermore, the standard deviation differs and varies between 1.2 % (4.0 kV/mm at 2000 V/s-ramp) and 16.8 % (44.0 kV/mm at 50 V/s-ramp) for the setup B and between 3.1 % (5.3 kV/mm at 10 V/s-ramp) and 23.1 % (43.6 kV/mm at 500 V/s-ramp) for setup A, respectively. For the two-electrode setup B the breakdown strength increases with increasing voltage ramps – from 202.2 kV/mm up to 350.2 kV/mm (73 % increase). This trend is the same for the three-electrode setup A but on al lower level – from 150.4 kV/mm up to 257.0 kV/mm and strong scattering especially at faster voltage ramps. Only the values of the two fastest voltage ramps are significantly higher.

The same trend is observed for Glass B as shown in Fig. 3b) for the two setups A and B. Increasing breakdown strength with increasing voltage ramps is also found for Glass B – from 284.5 kV/mm up to 458.5 kV/mm and 214.9 kV/mm up to 344.6 kV/mm, respectively. There is almost no scattering ($\leq$ 2%) for the measurements with CSP-electrodes (setup B) whereas for the three-electrode setup A the standard deviation is between 4.0 % (13.4 kV/mm at 1000 V/s-ramp) and 21.5 % (46.2 kV/mm at 5 V/s-ramp).

An advantage of the CSP-electrodes (setup B) is that it is clearly visible by the naked eye where the breakdown went through the sample (Fig. 4). Therefore, with setup B a differentiation of the breakdown location is possible and shown for Glass A in Fig. 3c). It is obvious that the breakdown strengths values for breakdown within the electrode (blue) scatter much less ($\leq$ 6.5 %) than the ones at the electrode edge (red). Only the undifferentiated mixing of these two breakdown scenarios leads to an overall strong scatter of the breakdown strength. Additionally, breakdown within the electrode area seems less influenced by the voltage ramp. While the electrode edge breakdown strength shows a continuous increase with increasing voltage ramp, breakdown voltages from channels inside the electrode are almost on a plateau value of approximately 320 kV/mm. The values for the two slowest ramps appear lower but they are not statistically significant (two-sample t-test, $\alpha = 0.05$). Only the measured breakdown strength at the fastest ramps of 5000 V/s and 10,000 V/s show a significant higher level. Another observation is that the ratio between breakdown within the electrode area and at the electrode edge changes with voltage ramp – at 5 V/s all breakdown events occurred at the electrode edge while up to 2000 V/s the percentage of breakdowns within the electrode area

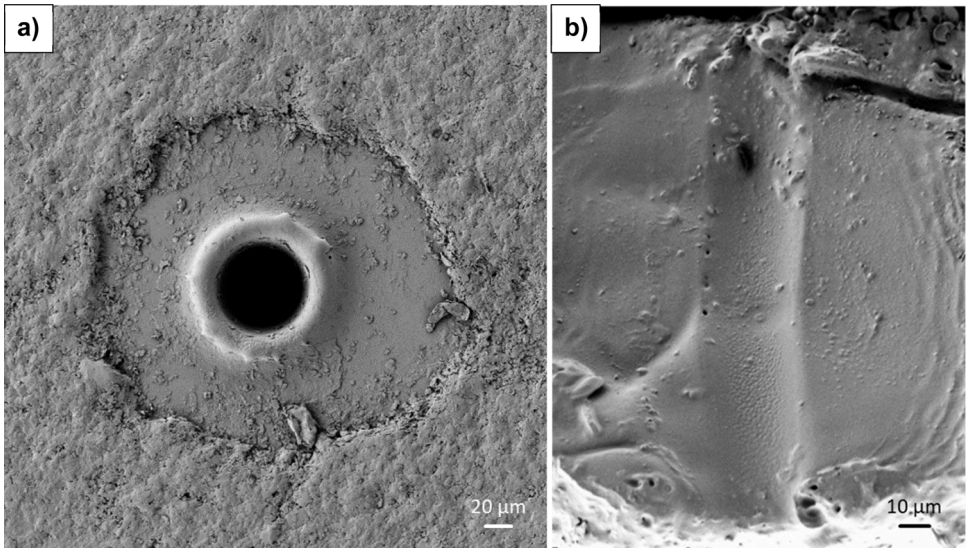

Fig. 2. SEM image of breakdown channels in Glass A. a) shows the „black spot "within the CSP-electrode. Around the entry hole of the breakdown the CSP is burnt away. In b) the cross section of such a breakdown channel through the sample is shown.

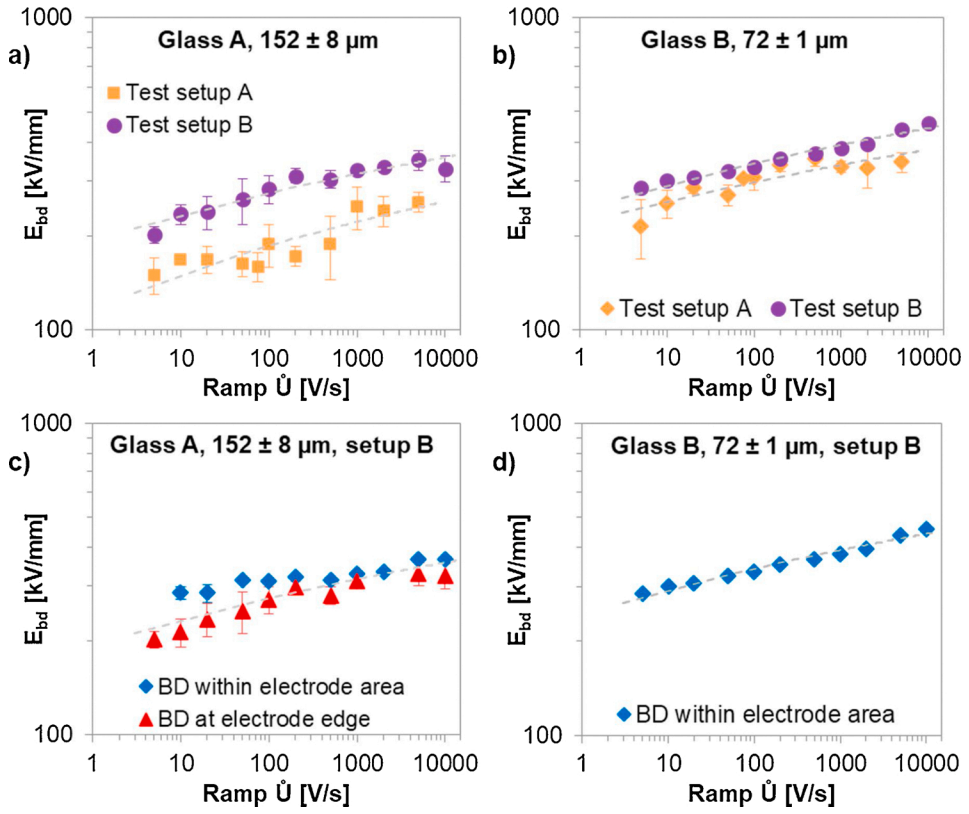

Fig. 3. Dielectric breakdown strength of Glass A (left) and Glass B (right) versus applied voltage ramp. In a) a comparison of Glass A tested in setup A and setup B, respectively, is shown. In b) we see this comparison for Glass B. In c) and d) the breakdown measurements with setup B are distinguished according to the location of the breakdown channel – within the electrode area or at the edge of the CSPelectrode.

increases up to 100 %. All breakdown events were initiated within the electrode area. With even faster ramps the probability of edge breakdown increases again.

Fig. 2d) shows the same differentiation between the locations of breakdown channel for Glass B in setup B. Here, all breakdown events were initiated within the electrode area of the CSP-electrodes, which is also the reason why the scattering is so low. But although the breakdown was initiated each time within the electrode area, there is a continuous upward trend with increasing voltage ramp.

For comparison the dielectric breakdown strength of alumina was tested with setup B at three different voltage ramps, 5 V/s, 200 V/s and 2000 V/s, and is plotted in Fig. 5. The breakdown was always initiated within the electrode area and the standard deviation is between 4.7 % (at 200 V/s) and 13.1 % (at 2000 V/s). The mean values rise from 52.3 ± 5.4 kV/mm to 58.7 ± 2.8 kV/mm at 200 V/s-ramp, which is an statistically significant difference (two-sample t-test, $\alpha = 005$), but then drops

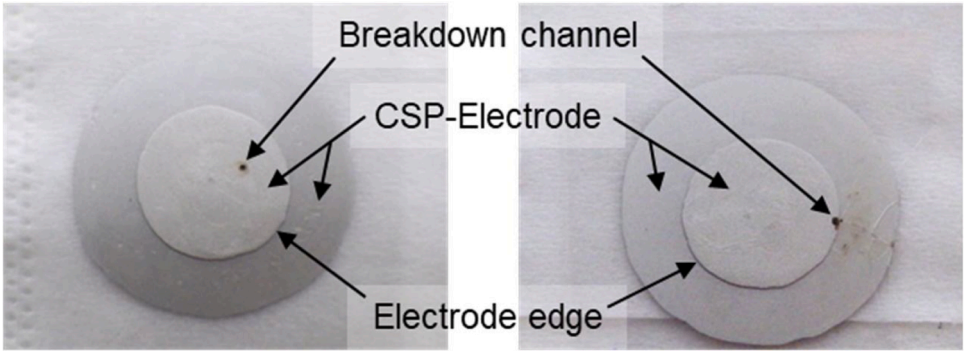

Fig. 4. Breakdown channel within the electrode area (left) and breakdown channel at the electrode edge (right).

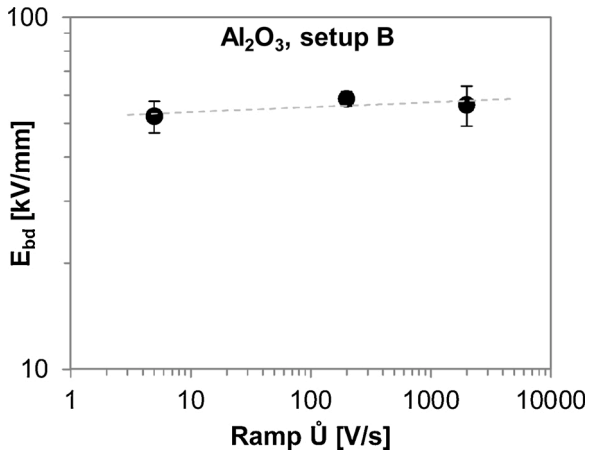

Fig. 5. Dielectric breakdown strength of alumina (d = 503 ± 15 µm) measured with CSP-electrodes under test setup B at three different voltage ramps. All breakdown events were initiated within the electrode area. Plotted are the arithmetic mean values with standard deviation of minimum 5 measurements.

slightly again to 56.4 ± 7.4 kV/mm at 2000 V/s-ramp, which is, however, not significant. Also comparing the breakdowns strength of 5 V/s and 2000 V/s there is no significant difference.

In Fig. 6 comparative measurements with the different electrode configurations of the ASTM and DIN standard were conducted to assess the results of our setups. The measurement setup C according to ASTM [43,44] with two opposing rod-electrodes showed the usual high scattering and a significantly lower value for the dielectric breakdown strength than with the other electrode configurations. The setup according to the German Standard [41,42] was conducted at two different voltage ramps. 5000 V/s is recommended by the standard, so the

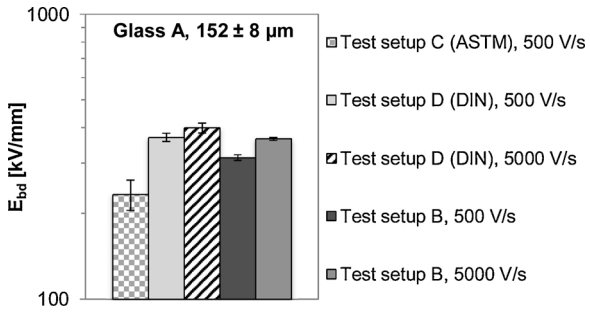

Fig. 6. A comparison of the breakdown strength of Glass A measured with different electrode setups at 500 V/s and 5000 V/s. The test setup C at 500 V/s is in agreement with the ASTM and the test setup D at 5000 V/s is in agreement with the DIN standard.

breakdown occurs between 10 and 20 s, and 500 V/s was chosen for comparison with the other results. A ball electrode paired with a cylinder electrode as recommended in the standards lead to high levels of dielectric breakdown values. The obtained dielectric breakdown strength is 17.8 % and 9.3 % higher, respectively, than the ones with the CSP-electrodes (setup B). However, it is difficult to say whether only the breakdown through the glass substrate was measured or whether the dielectric strength of the oil also influences the ASTM and DIN test. If no conductive silver paste is used, but only electrodes are placed on the sample, an oil layer between electrode and sample must always be assumed.

4. Discussion

Different dielectric breakdown strengths were measured for the same material due to different measurement conditions. The velocity at which the dielectric breakdown tests are carried out has an influence on how high the dielectric strength is measured. Also the electrode configuration has a strong impact not only on the level of breakdown strength but also on the scattering of the results. So far this is in agreement with the common accepted findings [37,40–44]. But although it is widely accepted, little attention is paid to it.

For the determination of the dielectric strength there are similar standards from various institutions (e.g. DIN, ASTM, BSI), which contain specific requirements on electrode shape and size and in the DIN EN 60243−1:2014−01 it additionally stipulate that the voltage ramp should be selected so that the breakdown occurs within 10–20 seconds. These specifications are useful to provide a standardized measurement method in the attempt that the results – for e.g. competitive materials – from the same test setup are comparable. Nevertheless, the data show, e. g. recently by Mieller 2019, that even within the framework of these standards differences in the dielectric breakdown strength of up to 50 % could be achieved with the same material [40]. This demonstrates the importance of having a comprehensive view on the mechanism of the dielectric breakdown and to record as much parameters as possible and to communicate this information in the publications. This objective of this work is not about generating norm-compliant data, but rather acquiring a deeper understanding of dielectric breakdown mechanism by reducing the effects of the experimental test conditions insuring that the breakdown is triggered by the material itself.

The results obtained here confirm that the speed of the voltage ramp and the electrode geometry have a strong impact on the dielectric strength. It is very surprising how strong this effect is: For one and the same material, results deviating by up to 143 % were measured. The lowest value for Glass A is 150 kV/mm and the highest is 365 kV/mm. The same is true for Glass B, where there is a 113 % difference between 215 kV/mm as the lowest value and 458 kV/mm as the highest value.

If the ASTM and DIN standard measurements are not considered, the lowest values were measured with the three-electrode arrangement (setup A) at the slowest voltage ramp, while the highest values were

measured with the CSP electrodes (setup B) and at the fastest voltage ramp. Taking the standardized measurements into account, an even 9% higher value of 399 kV/mm is measured for Glass A using the "ball on plate" setup. This indicates that conductive silver electrodes influence the measured dielectric strength. On the other hand if electrodes are applied by touching the samples' surface (force controlled) and additionally using insulating oil it is unclear how much the dielectric strength of the oil layer influences the measurement by a discharge inside the oil. From the work of Talbi et al. and Neusel at al. [56,57] we know that most likely space-charge limited conductivity right before breakdown is the dominant conductivity mechanism and not linear ohmic conductivity. Nevertheless, we use a simple dielectric model to estimate the electric field $E_{oil} = \frac{U}{s_{oil}+s_{glass}\cdot\frac{\varepsilon_{oil}}{\varepsilon_{glass}}}$ within the thin oil layer in a planar capacitor geometry with the oil thickness s_{oil} and permittivity ε_{oil} and the glass thickness s_{glass} and permittivity ε_{glass}. Correspondingly, the electric field in the glass is $E_{glass} = \frac{(U-E_{oil}\ s_{oil})}{s_{glass}}$. As an example, the case is calculated in Fig. 7 for glass A. We used the data we gained from test setup B at a voltage ramp of 200 V/s. It can be seen that the electric field within the glass substrate decreases with increasing oil film thickness and the field strength within the sample is lower than its dielectric breakdown strength for oil layer thickness greater than 4 µm. Additionally, the dielectric strength of the insulating oil is achieved with oil layer thicknesses of approximately 16 µm and less. This means that the oil layer is favorable to fail and measurements involving an oil layer are very likely to breakdown in an undefined state. As a consequence, a discharge is initiated in the oil layer, which in turn could lead to a temporarily conducting channel in the oil and thereafter to a breakdown in the glass. Even though this calculation differs from the actual geometry of the tests and space charge conductivity is not taken into account it qualitatively shows the oils' influence on the measurement.

With the ball-on-plate electrode (DIN, setup D), the distance between the surface of the upper ball electrode and the substrate increases with the distance from the point of contact. So with this electrode configuration the initiation of the dielectric breakdown depends a lot on the insulating oil. If the breakdown is not initiated directly at this contact point, the occurance/event is undefined. Our experience is that it initiates rather seldom directly at the point of contact.

All of this leads us to the conclusion that the breakdown should not run through the oil because otherwise it is difficult or impossible to make a qualitative statement about the triggering mechanism of the dielectric breakdown. The electric field distribution is strongly inhomogeneous and it is not possible to determine at which local electric field the breakdown started. In our opinion only electrodes on plan-parallel sample surfaces together with the "post-mortem" identification of the breakdown channel being inside the electrode area physically guarantee well defined breakdown conditions, which can be used to interpret the breakdown mechanism.

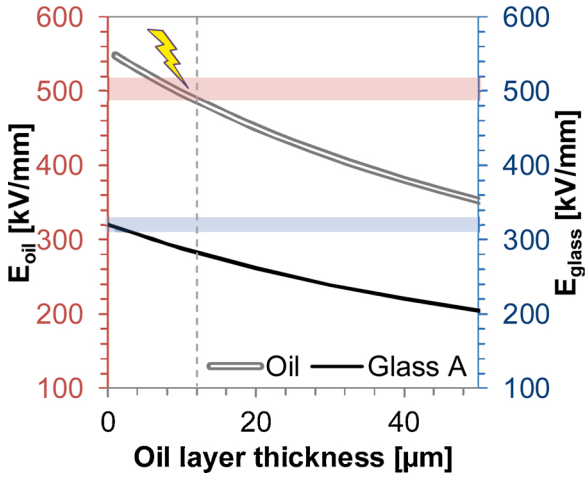

Fig. 7. Electric field strength within Glass A and the oil layer, respectively, as a function of the oil layer thickness. The blue area marks the range of dielectric strength of Glass A tested with setup B at 200 V/s, the red area marks it for the insulating oil. Exemplarily calculated with the average breakdown voltage of Glass A, 48.6 kV, and the average thickness of the corresponding samples, 151.4 µm (For interpretation of the references to colour in this figure legend, the reader is referred to the web version of this article).

Another advantage of the silver electrodes is that the breakdown channel is clearly visible for the naked eye and thereby the samples and their breakdown strengths could be divided in two groups: the ones where the breakdown occurred within the electrode area and the ones where the breakdown was initialized at the electrode edge. By doing so, two different behaviors could be identified as seen in Fig. 3. The breakdowns within the electrode area are quite impassible by the voltage ramp, only the results for 20 and 10 V/s are significantly lower and for 5000 V/s and 10,000 V/s significantly higher. The same pattern is also shown by the standard deviation, which is overall very low, but is about twice as large with 4.5%–6.5% for the two slowest ramps (the 5 V/s-ramp does not appear in the diagram, because at this voltage ramp all breakdowns have occurred at the edge of the electrode). We interpret this is an indication that the measurement setup with the CSP-electrodes leads to a sufficiently homogeneous electric field within the sample. Thus, a measurement, which is as little affected by external influences as possible, could be carried out.

The standard deviations, which are generally quite high for breakdown values, also show a large difference: For breakdowns at the electrode edge the standard deviation is on average 9% (22 kV/mm) whereas for breakdown inside the electrode the standard deviation is on average 3% (8 kV/mm). To investigate this phenomenon in more detail 12 additional measurements at a voltage ramp rate of 200 V/s were conducted giving 22 data point in total. The determined dielectric breakdown strength values were divided in two groups of "breakdown within the electrode area" (13 samples) and "breakdown at the electrode edge" (9 samples). The Weibull-plot of these results is shown in Fig. 8. The values from the electrode edge show a poor fitting to the reference line with a slope of m = 15, which is the Weibull modulus. For the data points from the electrode area the Weibull modulus is m = 67. The result that breakdowns within the electrodes arise at much higher voltages with much less scatter of the breakdown strength is confirmed.

In addition it is possible to analyze the probability of the breakdown initiating within the electrode area or at the edge. As shown in Fig. 9 the likelihood for the breakdown to occur at the electrode edge increases with decreasing voltage ramp rate. While at a voltage ramp rate of 2000 V/s all the samples broke down within the electrode area, not a single one did at a voltage ramp of 5 V/s. The shift happened between 100 V/s and 200 V/s. With even faster ramps, however, the probability of an edge breakdown increases again. Either a new range/zone (different time dependency, mechanism, etc.) is reached or it is due to the device and its limitations. Up to a voltage ramp of 2 kV/s set voltage and actual voltage coincide. At a voltage ramp of 5 kV the actual voltage is 1 kV behind the set voltage and at a voltage ramp of 10 kV it is 2.2 kV behind. Thus, we reach the limits of our test equipment.

At a voltage ramp of 200 V/s also 151.7 ± 3.1 µm and 213.7 ± 5.4 µm thick Glass B was tested. Here, we were interested in the location of the breakdown channel. The results are given in Fig. 9 as the probability of the breakdown initializing within the electrode area and the breakdown initializing at the electrode edge. As mentioned before, for the 70 µm thick Glass B the breakdown always occurred within the electrode edge. For the 150 µm thick Glass B 8 out of 10 samples broke down within the electrode area and two at the edge and for the 210 µm thick Glass B the breakdown always occurred at the electrode edge, even at a voltage ramp of 5000 V/s.

For 72 µm thick Glass B the influence of the voltage ramp is stronger. In contrast to Glass A all breakdown events were initialized within the electrode area and, however, the breakdown strength deceases with

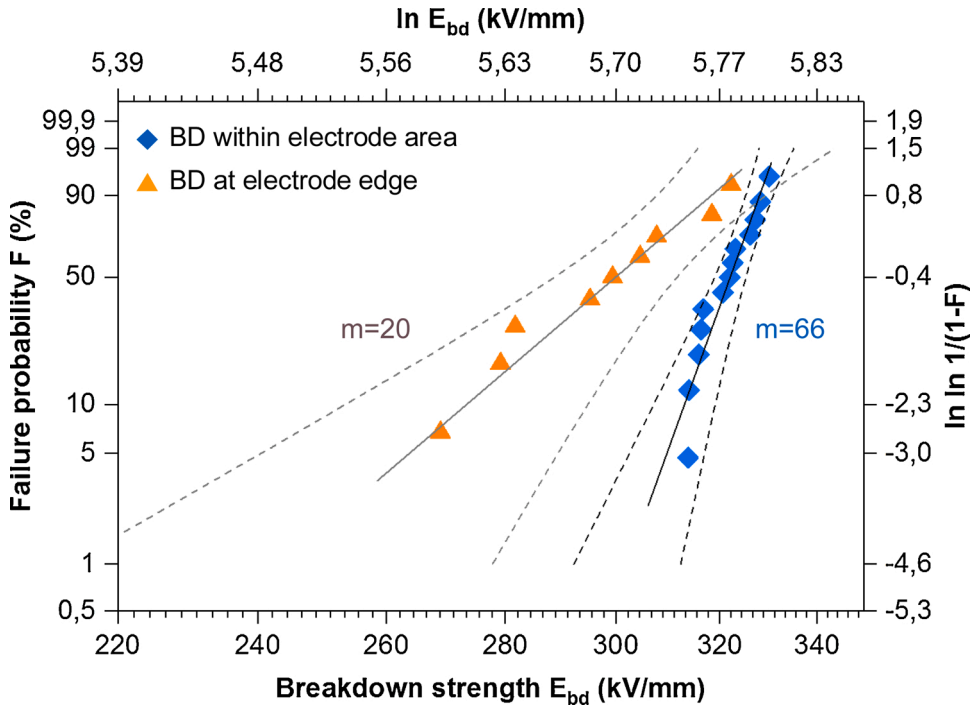

Fig. 8. Weibull plot of the breakdown voltage at a 200 V/s-ramp for Glass A, 152 µm, measured with test setup B. The results distinguished in regard of the breakdown location at the edge of the electrode or within the CSP-electrode area. Weibull moduli m and 95 % confidence intervals are included as dashed lines.

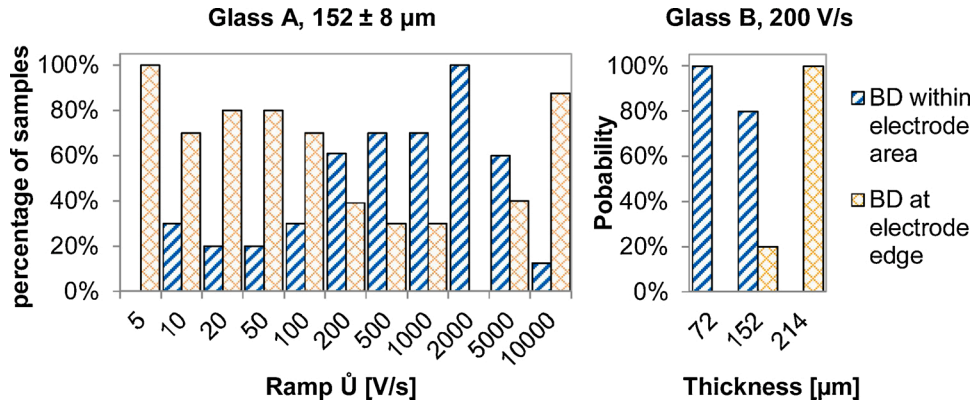

Fig. 9. Left: Correlation of ramp rate and initialization point of breakdown. With lower voltage ramp the breakdown tends to occur at the electrode edges which leads to misleading results for the breakdown strength and should not be taken into account for the determination of the breakdown strength of a material. Right: Probability of the breakdown location depending on the material thickness.

decreasing voltage ramp. But if we normalize the results to the thickness and permittivity of Glass A the trend of both investigated glasses looks similar as shown in Fig. 10.

For the 214 µm thick Glass B the weak spots were always at the electrode edge. If we assume that there are no defects within the samples and the surface filaments have the same length as the ones in thinner samples, the impact of these filaments is much bigger in thin samples than in thicker ones. From our publication [58] we can estimate the filaments to be around 20–30 µm long. This corresponds to up to 40 % of the 72 µm thick sample. With increasing material thickness this ratio is shrinking and thus the breakdown at the electrode edge becomes more likely (Fig. 11).

It is obvious that the edge of the electrode represents a favored breakdown location/line, as margins, edges and corners cause field enhancements (hence the rounded electrode shape in the standards or the Rogowski-profile). Jagged edge geometries from SEM images support this hypothesis and show a radius of curvature of the conductive

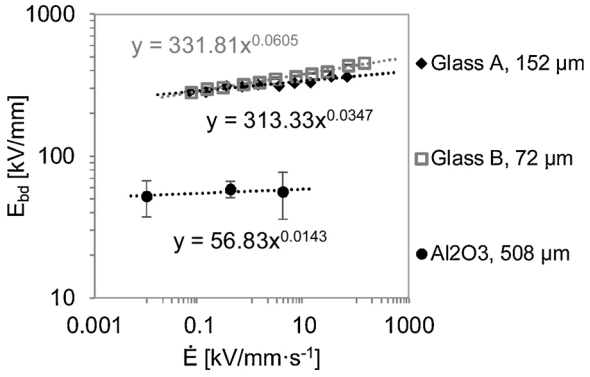

Fig. 10. Dielectric breakdown strength as a function of the electric field ramp of Glass A, Glass B and AO under test setup B. From the slope of the regression line the parameter n can be calculated.

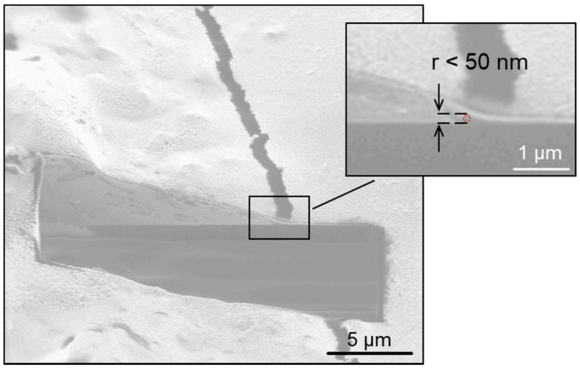

Fig. 11. FIB picture of the edge of a conductive silver paint electrode. By FIB a cross section was removed to have a look inside to see the radius of curvature.

silver at its outer edge <50 nm Under these circumstances/considerations, data derived from edge breaches should not be included, as undefined conditions prevail here.

The location of the breakdown is not just by chance but is influenced by the voltage ramp. With slower ramps the breakdown tends to initialize at the electrode edge. Additionally, the values from the electrode edge show a strong downward trend with the decreasing ramp. An explanation for this phenomenon could be the slow extension of the filaments of length a due to local charge accumulation. With slower voltage ramps and thus associated longer exposure time this effect becomes stronger, which we see in a drop of 35.3 % of dielectric strength from 312.6 kV at 1000 V/s to 202.2 kV at 5 V/s (the 2000 and 5000 V/s-ramps do not appear here, because at this ramp all breakdowns have occurred within the electrode area). If we assume a subcritical filament growth velocity v similar to subcritical crack growth [59] by a power-law:

$$v = \frac{da}{dt} = A\, G_{bd}^{n} \tag{1}$$

Where A and n are materials constants and G_{bd} is the energy release rate for a breakdown channel under applied electric field E_{appl} as defined in Schneider [28].

$$G_{bd} = b\, \varepsilon\, \varepsilon_0\, E_{appl}^2 a\, d \tag{2}$$

where ε *and* ε_0 are the dielectric constant of the insulator and the permittivity of free space, d is the thickness of the sample and b a geometrical constant. Putting (1) and (2) together we get:

$$dt = \frac{1}{A\,(b\, \varepsilon\, \varepsilon_0\, E_{appl}^2 a\, d)^n} da \tag{3}$$

Integration of (3) from the initial filament length a_i to the critical value a_c yields for an arbitrary time dependent applied electric field $E_{appl}(t)$

$$\int_0^{t_{bd}} E_{appl}^{2n}(t)dt = \frac{1}{A(\,\varepsilon\, \varepsilon_0\, d)^n (n-1)} \left[a_i^{1-n} - a_c^{1-n}\right] \tag{4}$$

If it is assumed that the lifetime t_f and breakdown strength E_{bd} are caused by the same initial filaments, the initial breakdown strength E_i as well as the final breakdown strength can be calculated as follows:

$a_i = \frac{G_{bd}^c}{b\, \varepsilon\, \varepsilon_0\, d\, E_i^2}$ and $a_c = \frac{G_{bd}^c}{b\, \varepsilon\, \varepsilon_0\, d\, E_{bd}^2}$ (5a and b)

Introducing (5) into (4) leads to

$$\int_0^{t_{bd}} E_{appl}^{2n}(t)dt = \frac{1}{A(\,\varepsilon\, \varepsilon_0\, d)^n (n-1)}\, E_i^{n-1}\left(1 - \left(\frac{E_{bd}}{E_i}\right)^{n-1}\right) \tag{6}$$

Combining material parameters and defining a new parameter B as

$$B = \frac{1}{A(\,\varepsilon\, \varepsilon_0)^n (n-1)} \tag{7}$$

We finally get:

$$\int_0^{t_{bd}} E_{appl}^{2n}(t)dt = \frac{B}{d^n}\, E_i^{n-1}\left(1 - \left(\frac{E_{bd}}{E_i}\right)^{n-1}\right) \tag{8}$$

In our experiments constant voltage ramps $\dot{U}$ corresponding to constant loading rate of the applied electric field $\dot{E} = const$ were used. Hence $E_{appl} = \dot{E}t$ and the integral on left hand side of (9) can be solved analytically, leading to the result:

$$E_{bd}^{2n+1} = \dot{E}(2n+1)\frac{B}{d^n}\, E_i^{n-1}\left(1 - \left(\frac{E_{bd}}{E_i}\right)^{n-1}\right) \tag{9}$$

For $n \gg 1$, $\left(\frac{E_{bd}}{E_i}\right)^{n-1} \ll 1$ and (9) can be approximated by:

$$E_{bd}^{2n+1} = \dot{E}(2n+1)\frac{B}{d^n}\, E_i^{n-1},\ for\ n >> 1 \tag{10}$$

In the logarithmic form (10) reads:

$$\ln E_{bd} = \frac{1}{2n+1}\ln\dot{E} + \frac{1}{2n+1}\ln\left[(2n+1)\frac{B}{d^n}\, E_i^{n-1}\right],\ for\ n >> 1 \tag{11}$$

Exactly this relationship for all samples with setup B is plotted in Fig. 9 for normalized values of a thickness $d = 152\ \mu m$. The evaluation of the slope in this double logarithmic plot leads to the n values as given in Table 3.

As can be seen in Table 3 the n-values are all much bigger than 1. n-values for subcritical crack growth at room temperature for alumina ceramics are 12–60 [60–62] and for borosilicate glass 15–50 [63–66]. These values have to be halved as the fracture mechanics n-values are related to the fracture toughness and the dielectric breakdown values are related to the breakdown toughness, $G \propto K^2$. The result shows that the parameter n for subcritical filament is similar in magnitude as the subcritical crack growth parameter.

5. Conclusion

As expected we found a clear dependence of the dielectric breakdown strength of the applied voltage ramp. With decreasing voltage ramp the breakdown strength decreases. Additionally, the scattering increases with lower voltage ramps. Another important finding was the importance of the conductive silver paint electrodes for our measurements. When the same measurements were carried out with and without conductive silver paint electrodes it turned out, that the breakdown strength values are significantly lower without CSP-electrodes and the scattering is very high. Thus, the surrounding insulating medium has a great impact on the breakdown strength measurement of a material. If partial discharge or flash over is happening during the measurements, the breakdown strength will be significantly lower due to surface damage and related energy release.

To evaluate the dependence of the breakdown strength on the voltage or electric field loading rate, a model based on the hypothesis of subcritical filament growth was developed, which is very similar to the evaluation of subcritical crack growth data in ceramics. This model is able to describe the measured loading rate depending breakdown strengths data, which deliver a parameter for the subcritical filament

Table 3
Determined n-values for subcritical filament growth from Fig. 9 according to (11) for a normalized breakdown strength of all samples of = 152 µm.

Material	Glass A	Glass B	Al2O3
Subcritical filament growth value, n	13.9	7.8	34.5

growth. The analyzed subcritical filament growth parameters are similar to the determined subcritical crack growth parameter for the same ceramics.

It is very important to identify the breakdown locations because our measurements show that the breakdown at lower voltage ramps tends to be initiated at the edge of the electrode. This knowledge is fundamental for the interpretation of the measured breakdown strength. Previously, it was assumed that the breakdown strength scatters so much due to material properties or imperfections, respectively. Our results reveal however, that the scattering of the breakdown strengths values is due to the set-up and the way the breakdown measurement is conducted.

It is therefore of utmost importance to know the limitations of the measurement set-up. Questions about the disruptive potential gradient or the discharge voltage should be clarified in advance. It is also recommended to carry out measurements at lower material thicknesses in order to stay below this limit (if one is interested in the dielectric strength of the material). Measurements at different material thicknesses, which remain below the flashover voltage in oil or other surrounding media, can be scaled up with the $\frac{1}{\sqrt{d}}$ -dependency. This relationship has already been demonstrated in various publications [49, 67–70].

Declaration of Competing Interest

The authors declare that they have no known competing financial interests or personal relationships that could have appeared to influence the work reported in this paper.

Acknowledgements

This work was supported by the German Research Foundation (Deutsche Forschungsgemeinschaft, DFG) under project number SCHN-372/17-2 and SFB 986.

References

[1] A.v Hippel, Z. Physik 68 (1931) 309–324, https://doi.org/10.1007/BF01390864.
[2] A.v Hippel, Z. Physik 67 (1931) 707–724, https://doi.org/10.1007/BF01390754.
[3] A.v Hippel, Z. Physik 75 (1932) 145–170, https://doi.org/10.1007/BF01341768.
[4] H. Fröhlich, Rep. Prog. Phys. 6 (1939) 411–430, https://doi.org/10.1088/0034-4885/6/1/326.
[5] H. Fröhlich, B.V.V. Paranjape, Proc. Phys. Soc. B 69 (1956) 21–32, https://doi.org/10.1088/0370-1301/69/1/304.
[6] V. Fock, Archiv f. Elektrotechnik 19 (1927) 71–81, https://doi.org/10.1007/BF01656306.
[7] P.H. Moon, Trans. Am. Inst. Electr. Eng. 50 (1931) 1008–1021, https://doi.org/10.1109/T-AIEE.1931.5055909.
[8] K.W. Wagner, Archiv f. Elektrotechnik 39 (1948) 215–233, https://doi.org/10.1007/BF01619168.
[9] K.H. STARK, C.G. Garton, Nature 176 (1955) 1225–1226, https://doi.org/10.1038/1761225a0.
[10] J.C. Fothergill, IEEE Trans. Dielectr. Electr. Insul. 26 (1991) 1124–1129, https://doi.org/10.1109/14.108149.
[11] N. Klein, H. Gafni, IEEE Trans. Electron Devices ED-13 (1966) 281–289, https://doi.org/10.1109/T-ED.1966.15681.
[12] J.J. O'Dwyer, J. Phys. Chem. Solids 28 (1967) 1137–1144, https://doi.org/10.1016/0022-3697(67)90057-1.
[13] J.J. O'Dwyer, Breakdown in Solid Dielectrics 1982 Annual Report: Conference on Electrical Insulation and Dielectric Phenomena : October 17-21, 1982, University of Massacusetts, Amherst, Massacusetts CONFERENCE ON ELECTRICAL INSULATION & Dielectric Phenomena — Annual Report 1982 (Amherst, MA), Institute of Electrical and Electronics Engineers, Piscataway, New Jersey, 1982, pp. 319–327, https://doi.org/10.1109/CEIDP.1982.7726551.
[14] M. Sparks, D.L. Mills, R. Warren, T. Holstein, A.A. Maradudin, L.J. Sham, E. Loh, D. F. King, Phys. Rev. B 24 (1981) 3519–3536, https://doi.org/10.1103/PhysRevB.24.3519.
[15] P. Budenstein, IEEE Trans. Dielectr. Electr. Insul. EI-15 (1980) 225–240, https://doi.org/10.1109/TEI.1980.298315.
[16] J.W. McPherson, R.B. Khamankar, A. Shanware, J. Appl. Phys. 88 (2000) 5351–5359, https://doi.org/10.1063/1.1318369.
[17] Y. Sun, C. Bealing, S. Boggs, R. Ramprasad, IEEE Electr. Insul. Mag. 29 (2013) 8–15, https://doi.org/10.1109/MEI.2013.6457595.
[18] Y. Sun, S.A. Boggs, R. Ramprasad, Appl. Phys. Lett. 101 (2012), 132906, https://doi.org/10.1063/1.4755841.
[19] S. Lin, H.G. Beom, D. Tao, Y.H. Kim, Fatigue Fract. Eng. Mater. Struct. 32 (2009) 580–586, https://doi.org/10.1111/j.1460-2695.2009.01362.x.
[20] T.-Y.-Y. Zhang, M.-H.-H. Zhao, C.-F. Gao, Int. J. Fract. Mech. 132 (2005) 311–327, https://doi.org/10.1007/s10704-005-2054-8.
[21] H.G.G. Beom, Y.H. Kim, Int. J. Solids Struct. 45 (2008) 6045–6055, https://doi.org/10.1016/j.ijsolstr.2008.07.020.
[22] T. Wang, T.-Y. Zhang, Appl. Phys. Lett. 79 (2001) 4198–4200, https://doi.org/10.1063/1.1427437.
[23] R. Fu, C.-F. Qian, T.-Y. Zhang, Appl. Phys. Lett. 76 (2000) 126–128, https://doi.org/10.1063/1.125678.
[24] H.R. Zeller, W.R. Schneider, J. Appl. Phys. 56 (1984) 455–459, https://doi.org/10.1063/1.333931.
[25] R.M. McMeeking, J. Appl. Phys. 62 (1987) 3116–3122, https://doi.org/10.1063/1.339361.
[26] Z. Suo, J. Mech. Phys. Solids 41 (1993) 1155–1176, https://doi.org/10.1016/0022-5096(93)90088-W.
[27] A. Vojta, D.R. Clarke, J. Appl. Phys. 83 (1998) 5632–5635, https://doi.org/10.1063/1.367415.
[28] G.A. Schneider, J. Mech. Phys. Solids 61 (2013) 78–90, https://doi.org/10.1016/j.jmps.2012.09.005.
[29] J. Liebault, J. Vallayer, D. Goeuriot, D. Treheux, F. Thevenot, J. Eur. Ceram. Soc. 21 (2001) 389–397, https://doi.org/10.1016/S0955-2219(00)00186-2.
[30] A. Si Ahmed, J. Kansy, K. Zarbout, G. Moya, J. Liebault, D. Gœuriot, J. Eur. Ceram. Soc. 25 (2005) 2813–2816, https://doi.org/10.1016/j.jeurceramsoc.2005.03.146.
[31] M. Touzin, D. Goeuriot, H.-J. Fitting, C. Guerret-Piécourt, D. Juvé, D. Tréheux, J. Eur. Ceram. Soc. 27 (2007) 1193–1197, https://doi.org/10.1016/j.jeurceramsoc.2006.05.047.
[32] L. Haddour, N. Mesrati, D. Goeuriot, D. Tréheux, J. Eur. Ceram. Soc. 29 (2009) 2747–2756, https://doi.org/10.1016/j.jeurceramsoc.2009.03.022.
[33] K. Zarbout, G. Moya, A.S. Ahmed, G. Damamme, A. Kallel, J. Appl. Phys. 108 (2010) 94109, https://doi.org/10.1007/s10854-016-5554-6.
[34] S. Laihonen, U. Gafvert, T. Schutte, U. Gedde, IEEE Trans. Dielectr. Electr. Insul. 14 (2007) 275–286, https://doi.org/10.1109/TDEI.2007.344604.
[35] I.O. Owate, R. Freer, Dielectric Breakdwon of Ceramics and Glass Ceramics: University of Manchester Institute of Science and Technology, UK (Conference Publication no. 363), The Institution, London, 1992. ISBN: 0-85296-551-556.
[36] A. Tröls, A. Kogler, R. Baumgartner, R. Kaltseis, C. Keplinger, R. Schwödiauer, I. Graz, S. Bauer, Smart Mater. Struct. 22 (2013), 104012, https://doi.org/10.1088/0964-1726/22/10/104012.
[37] A. Küchler, High Voltage Engineering, Springer Berlin Heidelberg), Berlin, Heidelberg, 2018, https://doi.org/10.1007/978-3-642-11993-4.
[38] E. Kuffel, W.S. Zaengl, J. Kuffel, High Voltage Engineering: Fundamentals, 2nd edn, Newnes Elsevier, Amsterdam, 2008. ISBN: 9780750636346.
[39] H.M. Ryan, High Voltage Engineering and Testing (The Institution of Engineering and Technology, Michael Faraday House, Six Hills Way, Stevenage SG1 2AY, IET, UK, 2001, https://doi.org/10.1049/PBPO032E.
[40] B. Mieller, J Adv Ceram 30 (2019) 1650, https://doi.org/10.1007/s40145-018-0310-4.
[41] Deutsches Institut für Normung Elektrische Durchschlagfestigkeit von isolierenden Werkstoffen - Prüfverfahren - Teil 1: Prüfungen bei technischen Frequenzen (IEC 60243-1:2013) (60243-1:2014-01).
[42] Deutsches Institut für Normung Elektrische Durchschlagfestigkeit von isolierenden Werkstoffen - Prüfverfahren - Teil 2: Zusätzliche Anforderungen für Prüfungen mit Gleichspannung (IEC 60243-2:2013) (60243-2:2014-08).
[43] American Society for Testing and Materials Standard Test Method for Dielectric Breakdown Voltage and Dielectric Strength of Solid Electrical Insulating Materials at Commercial Power Frequencies (D149 - 09, 2013, https://doi.org/10.1520/D0149-09R13.
[44] American Society for Testing and Materials Standard Test Method for Dielectric Breakdown Voltage and Dielectric Strength of Solid Electrical Insulating Materials Under Direct-Voltage Stress (D3755 - 14), DOI: 10.1520/D3755-14.
[45] F. Palumbo, C. Wen, S. Lombardo, S. Pazos, F. Aguirre, M. Eizenberg, F. Hui, M. Lanza, Adv. Funct. Mater. 30 (2020), 1900657, https://doi.org/10.1002/adfm.201900657.
[46] F. Forlani, N. Minnaja, J. Vac. Sci. Technol. 6 (1969) 518–526, https://doi.org/10.1116/1.1315671.
[47] D.J. Dumin (Ed.), Oxide Reliability: A Summary of Silicon Oxide Wearout, Breakdown, and Reliability (Selected Topics in Electronics and Systems v. 23), World Scientific Pub. Co), Singapore, River Edge, N.J, 2002, https://doi.org/10.1142/9789812778062_0001.
[48] Y. Taur, T.H. Ning, Fundamentals of Modern VLSI Devices, Cambridge University Press, 2013, https://doi.org/10.1017/CBO9781139195065.
[49] C. Neusel, G.A. Schneider, J. Mech. Phys. Solids 63 (2014) 201–213, https://doi.org/10.1016/j.jmps.2013.09.009.
[50] C. Neusel, H. Jelitto, D. Schmidt, R. Janssen, F. Felten, G.A. Schneider, J. Eur. Ceram. Soc. 32 (2012) 1053–1057, https://doi.org/10.1016/j.jeurceramsoc.2011.11.013.
[51] Z. Wang, Y. Hu, H. Lu, F. Yu, J. Non. Solids 354 (2008) 1128–1132, https://doi.org/10.1016/j.jnoncrysol.2007.01.099.
[52] Lima MMRA, R.C.C. Monteiro, M.P.F. Graça, M.G. Ferreira da Silva, J. Alloys. Compd. 538 (2012) 66–72, https://doi.org/10.1016/j.jallcom.2012.05.024.
[53] SCHOTT, *Data sheet: D 263® M Cover Glass*, 2011.
[54] Almatis Data sheet: CT 3000 SG Alumina Powder.
[55] labsolute Data sheet: Borosilicate glass 3.3 cover glass.
[56] F. Talbi, F. Lalam, D. Malec, J. Phys. D Appl. Phys. 40 (2007) 3803–3806, https://doi.org/10.1088/0022-3727/40/12/037.

[57] C. Neusel, H. Jelitto, G.A. Schneider, J. Appl. Phys. 117 (2015), 154902, https://doi.org/10.1063/1.4917208.
[58] P.-K. Fischer, G.A. Schneider, J. Eur. Ceram. Soc. 38 (2018) 4476–4482, https://doi.org/10.1016/j.jeurceramsoc.2018.05.036.
[59] D. Munz, T. Fett, Ceramics: Mechanical Properties, Failure Behaviour, Materials Selection (Materials Science Vol 36), 2nd edn, Springer, Berlin, 2001. ISBN: 9783642635809.
[60] T. Fett, D. Munz, J. Am. Ceram. Soc. 75 (1992) 958–963, https://doi.org/10.1111/j.1151-2916.1992.tb04166.x.
[61] S.M. Barinov, N.V. Ivanov, S.V. Orlov, V.J. Shevchenko, J. Eur. Ceram. Soc. 18 (1998) 2057–2063, https://doi.org/10.1016/S0955-2219(98)00116-2.
[62] M. Szutkowska, M. Boniecki, J. Mater. Process. Technol. 175 (2006) 416–420, https://doi.org/10.1016/j.jmatprotec.2005.04.030.
[63] S.M. Wiederhorn, Fracture Mechanics of Ceramics (1974), https://doi.org/10.1007/978-1-4615-7014-1.
[64] T. Fett, K. Germerdonk, A. Grossmller, K. Keller, D. Munz, J. Mater. Sci. 26 (1991) 253–257, https://doi.org/10.1007/BF00576060.
[65] S.J. Dill, S.J. Bennison, R.H. Dauskardt, J. Am. Ceram. Soc. 80 (1997) 773–776, https://doi.org/10.1111/j.1151-2916.1997.tb02897.x.
[66] M.M. Smedskjaer, M. Bauchy, Appl. Phys. Lett. 107 (2015), 141901, https://doi.org/10.1063/1.4932377.
[67] C. Neusel, H. Jelitto, D. Schmidt, R. Janssen, F. Felten, G.A. Schneider, J. Eur. Ceram. Soc. 35 (2015) 113–123, https://doi.org/10.1016/j.jeurceramsoc.2014.08.028.
[68] C. Neusel, G.A. Schneider, Dependence of the breakdown strength on thickness and permittivity: (ICSD) : June 30 2013- July 4, 2013 piscataway, N.J, 2013 IEEE International Conference on Solid Dielectrics (2013). DOI: 10.1109/ICSD.2013.6619786.
[69] I.O. Owate, R. Freer, J. Mater. Sci. 25 (1990) 5291–5297, https://doi.org/10.1007/BF00580163.
[70] D. Malec, V. Bley, F. Talbi, F. Lalam, J. Eur. Ceram. Soc. 30 (2010) 3117–3123, https://doi.org/10.1016/j.jeurceramsoc.2010.07.024.